Heat Transfer—Asian Research, **42** (6), 2013

Experimental Study on the Effect of Porous Medium on Performance of a Single Tube Heat Exchanger: A CO_2 Case Study

Mohammad Tarawneh,[1] AbedAlrzaq Alshqirate,[2] Khaleel Khasawneh,[1] and Mahmoud Hammad[3]
[1]Mechanical Engineering Department, The Hashemite University, Zarqa, Jordan
[2]Alshoubak University College, Al-Blqa' Applied University, Alsalt, Jordan
[3]Mechanical Engineering, University of Jordan, Jordan

An experimental study on single-phase laminar forced convection in a single porous tube heat exchanger is presented. Parametric studies are conducted for different inlet pressures, different mass flow rates, and different porosities to evaluate the effects of particle diameter and Reynolds number on the heat transfer and friction factor. The Nusselt number and friction factor are developed for efficient design of a porous heat exchanger based on the present configuration. Heat is transferred to the walls of the heat exchanger by natural convection mode. Gravel sand with different porosities is used as a porous medium during the tests. The flow of carbon dioxide as a working fluid in the porous medium is modeled using the Brinkman–Forchheimer-extended Darcy model. A dimensionless performance parameter is developed in order to be used in evaluating the porous tube heat exchanger based on both the heat transfer enhancement and the associated pressure drop. The study covers a wide range of inlet pressures (P_i), mass flow rates ($\dot{m}$), porosity of gravel sand (ε), and particle diameters (d_m) which ranged $34.5 \le P_i \le 43$ bars, $8*10^{-5} \le \dot{m} \le 16*10^{-5}$ kg/s, $34.9\% \le \varepsilon \le 44.5\%$, $1.25 \le d_m \le 5.15$ mm, respectively. This study revealed that a smaller particle diameter can be used to achieve higher heat transfer enhancement, but a larger particle diameter leads to a more efficient performance based on heat transfer enhancement. The average heat transfer coefficient of carbon dioxide decreases when the porosity increases.
 Heat Trans Asian Res, 42(6): 473–484, 2013; Published online 10 April 2013 in Wiley Online Library (wileyonlinelibrary.com/journal/htj). DOI 10.1002/htj.21059

Key words: porous medium, forced convection, heat exchanger, single phase flow, carbon dioxide

1. Introduction

There has been a growing interest in heat transfer enhancement using a porous medium and several studies have reported that the use of porous medium for heat transfer yields higher heat transfer performance than existing techniques such as a pinned-fin array or twisted tape inserts. Alshqirate et al. [1] studied the effect of heat exchanger size on two-phase heat transfer coefficient when CO_2 is used as a working fluid in porous media. Al-Tarawneh [2] studied the characteristics of CO_2 during condensation and evaporation processes in porous media when used as refrigerant. Abo-Hijleh and

Al-Nimr [3] investigated the effect of the local inertial term on the fluid flow in channels partially filled with porous material. Lee and Vafai [4] performed analytical characterization and conceptual assessment of solid and fluid temperature differentials in porous media. An investigation into the effect of porous medium on performance of a single-phase flow heat exchanger is adopted by Dehghan and Aliparast [6]. Hammad et al. [7] investigated the cooling of superheated refrigerants flowing inside tubes filled with porous media. They studied the heat transfer and pressure drop characteristics of carbon dioxide in porous media. Jiang et al. [8] conducted an experimental investigation on Pettersen et al. [12] who investigated the development of compact heat exchangers for CO_2 air-conditioning systems. Sheng-Chung Tzeng et al. [14] studied friction and forced convective heat transfer in a sintered porous channel with obstacle blocks. Teamah et al. [15] performed a numerical simulation of laminar forced convection in a horizontal pipe partially filled with porous material. They investigated numerically the effect of Reynolds and Prandtl numbers on laminar forced convection in a horizontal pipe partially filled with porous material. From the previous review the new experimental study in the present work is to investigate the effect of particle diameter, and Reynolds number on the heat transfer and friction factor during the cooling of super heated carbon dioxide in a single porous tube heat exchanger upon which the forced convective flow exists. Carbon dioxide has zero ozone depletion potential and a very low global warming effect and is a promising gas in refrigeration and air conditioning fields. In the present study, a porous tube containing a fluid-saturated sintered porous sand matrix, which is affected by the natural convection heat transfer mode on its walls, is used to perform a detailed study of the hydrodynamic and heat transfer of single-phase flow characteristics within a porous tube. The experimental results for pressure drop and heat transfer of carbon dioxide during the cooling process in a single porous tube are developed. The flow in the porous medium is modeled using the Brinkman–Forchheimer-extended Darcy model (Oosthuizen et al.) [11].

Nomenclature

A_i: heat exchanger internal surface area, m^2
A_p: cross-sectional area of the porous bed, m^2
A_T: total cross-sectional area of the porous tube, m^2
C: inertia coefficient
C_f: inertia coefficient
CO_2: carbon dioxide, Pa·s
DAS: data acquisition system
D_e: effective diameter, m
D_i: internal diameter, m
d_m: mean diameter, m
f: friction factor
h_i: heat transfer coefficient, $W/m^2 \cdot K$
K: permeability
K_a: apparent thermal conductivity, W/m·K
K_s: thermal conductivity of the solid material, W/m·K
L_g: length of cooling region, m
Nu: Nusselt number
P_b: barometric pressure
P_{in}: test section inlet pressure, kPa
P_{out}: test section outlet pressure, kPa

Pr: Prandtl number
Re: Reynolds number
V_g: vapor velocity, m/s

Greek Symbols

ε: porosity
ε_p: performance parameter
ΔP_g: vapor pressure drop, kPa
ρ_m: mean density, kg/m^3
μ_m: mean dynamic viscosity

Subscripts

exp: experimental
g: gas
m: mean value

2. Experiments

Experiment conditions

The cooling process of superheated CO_2 gas is performed inside a selected single porous tube heat exchanger. The experimental conditions were determined and heat exchangers were fabricated according to the specifications as shown in Table 1.

Experimental procedure

The schematic diagram of the test rig used during the experiments is shown in Fig. 1. In order to measure the outside wall surface temperature during cooling and condensation processes, the chest freezer inside air temperature, and the ambient temperature, K-type thermocouples were used during the experimental tests and connected to a module (32 channels), which is in turn plugged into the data acquisition system of a model SCXI 1000, manufactured by National Instruments Company. The well-known LAB VIEW software is used for the processing of the thermocouple signals. For each

Table 1. Experimental Conditions

Process	Cooling inside chest freezer at -28 ^{o} C until saturation.
Working fluid	CO_2
Mean diameter of the particles of the sand(d_m), (mm)	1.25, 1.8, 2.03, 2.7, 3.18, 4.2, 5.15
Permeability(κ), (m^2)	$4.65*10^{-12}$, $5.7*10^{-12}$, $8.2*10^{-12}$
Porosity of sand	34.9%,37%,39.8%,42.4%,43%,43.8%, 44.5%
Test section total length, (m)	4
Test section inlet pressure, (kPa)	3450, 3700 ,4000, 4300
Saturation temperature in (^{o}C)	-0.4, 2.27, 5.30, 8.15
Volume flow rate, (Liter / min)	4, 5, 6,7

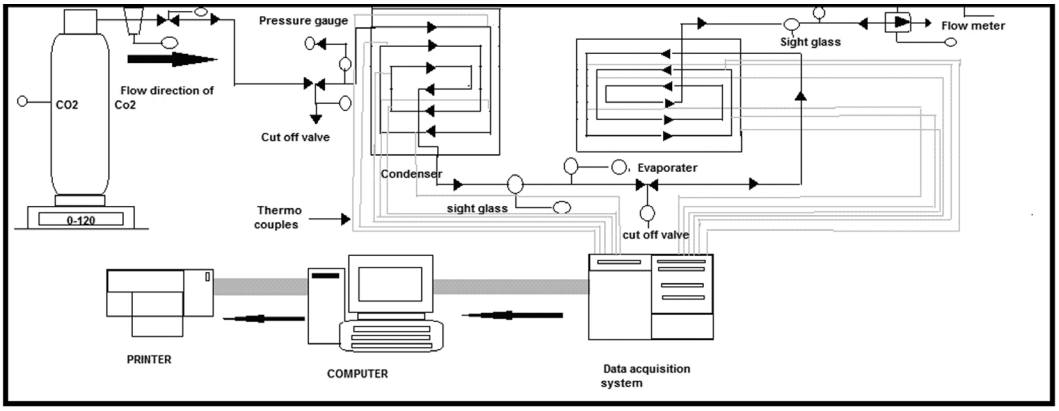

Fig. 1. Schematic diagram of the test rig.

experimental test run, the variation of the temperature with time can be monitored. The temperature readings are recorded repeatedly for a certain period until steady state conditions are achieved. The temperature readings were plotted against the length of the porous tube as shown in Fig. 2 for all test conditions. From this figure, it is clear that two lines with different slopes are shown; the first represents the sloped cooling line from 16.5 °C down to meet the second horizontal constant saturation temperature line at 6.5 °C. The length of the cooling portion of the pipe is shown. Distance on the x-axis is the length of the cooling tube. The experimental conditions used in this study are listed in Table 1. Local gravel sand that consists of 98% silica is prepared and cleaned in the lab in order to be used as a porous media. This material is readily available in the markets. From randomly selected samples, seven different grain size ranges were obtained and used.

3. Calculations

3.1 Apparent properties

In dealing with porous media it is preferred to use the apparent physical properties such as apparent thermal conductivity (K_a), apparent heat capacity (C_{pa}) and apparent viscosity (μ_a). The

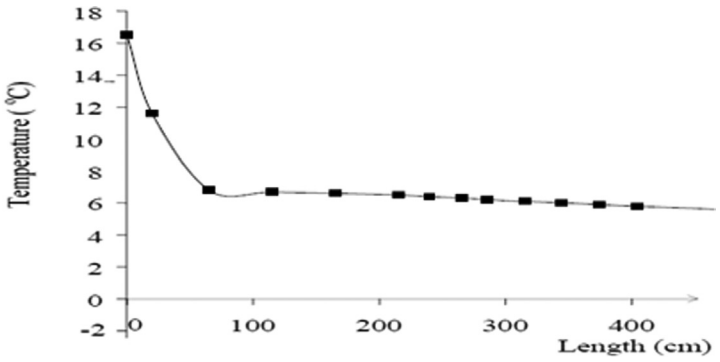

Fig. 2. Outside wall surface temperature (°C) versus porous tube test section length for inlet pressure = 4300 kPa, porosity = 39.8%, and mass flow rate = 16×10^{-5} kg/s.

above apparent physical properties can be calculated based on the effect of both solid material and fluid according to the following relations (Mills, 1995) [9]:

$$K_a = \varepsilon K_m + (1- \varepsilon) K_s \quad (1)$$

$$C_{pa} = \varepsilon C_{pm} + (1- \varepsilon) C_{ps} \quad (2)$$

while the apparent viscosity was enlarged due to the increase in its effect due to the increase in the contact area between the flowing fluid and the stationary porous media. It can be calculated by the following relation:

$$\mu_a = \gamma \mu_g \quad (3)$$

where $\gamma > 1$ and equals $[1 + (1 - \varepsilon)D_e/d_m]$, which is called the viscosity increase factor.

Thus, the apparent Reynolds number and Prandtl number can be calculated as follows:

$$Re_a = \rho V D_e / \mu_a \quad (4)$$

and

$$Pr_a = C_{pa} \mu_a / K_a \quad (5)$$

3.2 Heat transfer during the cooling process

To calculate what the experimental heat transfer coefficients (h_{exp}) were, the tube outside wall surface temperatures at 13 points along the whole test sections (about 4 m) were measured by means of K-type thermocouples fixed on the outer surface at longitudinal locations. These temperatures were tabulated along with the test section length. Two pressure values and the volumetric flow rate were tabulated as well. Different experiments were carried out changing independent variables: the porosity, ε (seven different values), the test section inlet pressure, P_{in} (four different values), and the flow rate, V (four different values). Figure 2 shows the pipe's longitudinal distribution of the outer surface temperatures of a typical cooling experiment. The figure shows a gas cooling part and a condensation part. The two lines have different slopes. The total length of the cooling and condensation portion was about 4 meters. This study is concerned only with the process of cooling. The length ranged from 0.4 to 0.7 m. For the cooling part of the pipe, the relation between the temperature and the pipe longitudinal distance is shown to be linear. A condition of constant heat flux can be assumed. Heat balance for the heat transfer inside the chest freezer will be as heat released by the gas while cooling by radial heat flux. Convection and conduction heat transfer will be considered as follows:

$$\dot{Q}_{CO2} = h_o A_o \Delta T_{lmo} \quad (6)$$

$$\dot{Q}_{CO2} = Cp_a (T1^{/} - T2^{/}) \quad (7)$$

$$\dot{Q}_{CO2} = h_i A_i \Delta T_{lmi} \quad (8)$$

where the outer logarithmic mean temperature difference equals:

$$\Delta T_{lmo} = [(T_1 - T_a) - (T_2 - T_a)] / \ln [(T_1 - Ta) / (T_2 - T_a)] \quad (9)$$

And the inner logarithmic mean temperature difference equals:

$$\Delta T_{lmi} = [(T_1'-T_1) - (T_2'-T_2)] / \ln [(T_1'-T_1)/(T_2'-T_2)] \quad (10)$$

where T_1 and T_2 are the first and last temperatures of the wall outside surface, T_1' and T_2' are the gas inlet and outlet mean temperatures, and T_a is the deep freezer air temperature.

Also, A_o and A_i are the outer surface tube area and the inner surface tube area, respectively, while h_o and h_i are the outer and the inner heat transfer coefficient, respectively.

Equation (6) will be used to calculate the heat quantity using the Churchill and Chue formula [5] to calculate h_o. The formula is:

$$Nu_D = \{0.60 + (0.387\ Ra_D^{1/6})/[1 + (0.559/Pr)^{9/16}]^{8/27}\}^2 \quad (11)$$

Equation (7) will be used to calculate the mean gas flow temperature at inlet (T_1') as the gas temperature at the exit is known to equal the saturation temperature at that pressure. Then Eq. (8) will be used to calculate the mean heat transfer coefficient of CO_2 at the inner surface flow of the tube. This will be the experimental heat transfer coefficient (h_{exp}) for the cooling of gaseous CO_2.

3.3 Pressure drop during cooling process

The inlet pressure (P_{in}) in kPa is measured and recorded. Then according to Forchheimer's extension of the Darcy model [11], which is valid for a laminar flow in a porous media, the cooling pressure drop of CO_2 can be calculated as follows:

$$\Delta p_g = \frac{(\mu_g v_g l_g)}{k} + C\rho_g l_g v_g^2 \quad (12)$$

where l_g, v_g, ρ_g, μ_g are the length (m) velocity of CO_2 vapor in m/s, density of CO_2 vapor in kg/m^3, and viscosity of CO_2 vapor in Pa·s, respectively. C is the inertia coefficient for spherical particles with mean diameter (d_m) [14] and is equal to

$$C = \frac{1.75((1-\varepsilon)}{\varepsilon^3 d_m} \quad (13)$$

The permeability κ of the porous media, which can be found according to Forchheimer's extension of the Darcy model, is valid for laminar flow in porous media according to the following relation:

$$k = \frac{(v_g l_g)}{A_p(\Delta p_g - C\rho l_g v_g^2)}\mu_g \quad (14)$$

where k is the permeability of the porous media (gravel sand) which is found experimentally according to the lab procedure of Ricardo and Fernands [13]. Then A_p is the cross-sectional area of the porous bed ($A_p = \varepsilon A_t$) (m^2) where A_T is the total cross-sectional area of the heat exchanger. The system geometry is represented by the effective diameter (D_e), which was defined by Mills [9] and Yoon et al. [16] as

$$D_e = d_m\left(\frac{\varepsilon}{1-\varepsilon}\right) \quad (15)$$

The apparent thermal conductivity (K_a) of the porous bed was used to represent the thermal conductivity of the complex porous bed which consists of the working fluid and the porous material. It is given by the following equations [16]:

$$K_a = \varepsilon K_g + (1-\varepsilon)K_s \tag{16}$$

where K_g is the thermal conductivity of the gaseous CO_2 and K_s is the thermal conductivity of the solid material (gravel). It is preferred to use highly thermally conductive solid materials as porous inserts. The Reynolds number based on the effective diameter (D_e) is calculated according to Mills [9] as follows:

$$\mathrm{Re}_{De} = \rho_g \times u_g \times d_m \times \varepsilon \big/ \mu_g (1-\varepsilon) \tag{17}$$

The friction factor (f) is calculated according to the cooling pressure drop (Δp_g) of the porous tube [6] as follows:

$$f = -\Delta p_g \frac{D_e}{\rho_g u_g{}^2 l_g} \tag{18}$$

4. Results and Discussion

The results of the study of flow and heat transfer in a single-tube heat exchanger completely filled with porous material (gravel and sand) will be introduced. The study covers a wide range of inlet pressure (P_i), mass flow rate ($\dot{m}$), particle diameter (d_m), and porosity of sand (ε) which ranged from: $34.5 \le P_i \le 43$ bars, $8*10^{-5} \le \dot{m} \le 16*10^{-5}$ kg/s, $1.25 \le d_m \le 5.15$ mm, $34.9\% \le \varepsilon \le 44.5\%$, respectively. In addition, parametric studies are also conducted to evaluate the effects of particle diameter, Reynolds number, and porosity on the heat transfer and pressure drop.

4.1 Effect of particle diameter on the friction factor (pressure drop)

To investigate the effects of particle diameter on the friction factor and pressure drop, the particle diameter is plotted against the friction factor and the pressure drop. It is shown in Figs. 3 and 4 that in the relatively small particle diameter region (Darcy regime), the length-averaged Nusselt number (Nu) (based on the effective diameter of the porous tube heat exchanger) and the pressure drop decreased sharply with an increasing d_m. For a large particle diameter (non-Darcy regime), the friction and the corresponding pressure drop both decrease slowly as they approach their corresponding asymptotic values for the nonporous case.

4.2 Effects of Reynolds number and the particle diameter on heat transfer

The combined effects of the Reynolds number and the particle diameter on heat transfer are illustrated in Fig. 5. As the Reynolds number is increased, the Nusselt number increases, and the porous medium with a smaller particle diameter generates a higher increase in heat transfer enhancement than one with a larger particle diameter. However, as the Reynolds number becomes smaller, the Nusselt number approaches an asymptotic value which is mainly dependent on the particle diameter. As expected, the average heat transfer coefficient increases when Re increases. This is due to the fact that the increase in Re increases the thermal entrance length, as known, the heat transfer in the entrance is high. Also it can be noticed that when the porosity of the sand decreases the heat transfer

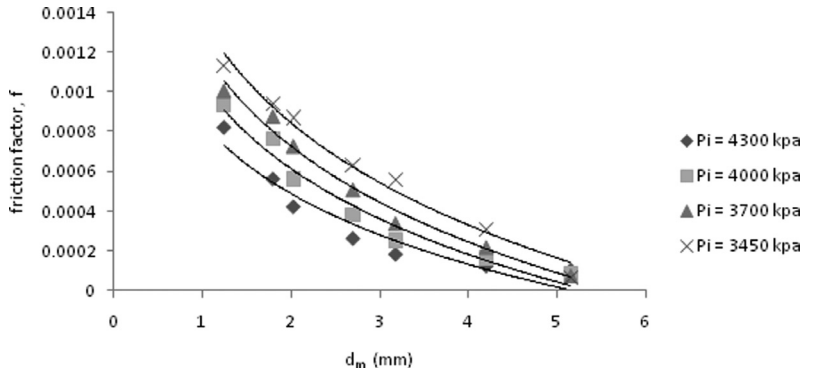

Fig. 3. Effect of particle diameter on the friction factor for different inlet pressures.

increases. This is due to the fact that as the porosity decreases (small particle diameters) the apparent thermal conductivity increases and accordingly the heat transfer rate increases.

4.3 Effects of particle diameter on heat transfer and pressure drop

It is clear from this investigation that a higher heat transfer rate is achieved at a larger penalty in pressure drop. Figures 4 to 6 show that both the Nusselt number and pressure drop increase as the particle diameter decreases. Also it is noticed that the increasing rates of both parameters are different and a relatively large penalty for the pressure drop will occur when a smaller particle diameter is selected to enhance the heat transfer. The increase in pressure drop is compensated for with the high heat transfer rates.

4.4 Effect of porosity on the average heat transfer coefficient

The effect of the gravel sand porosity is presented in Fig. 7 for different inlet pressures. As expected, the average heat transfer coefficient decreases when the porosity increases. This is due to the fact that the increase in porosity reduces the conduction heat transfer surface area between the fluid and the gravel sand and between the sand particles. Also it can be noticed that when the porosity

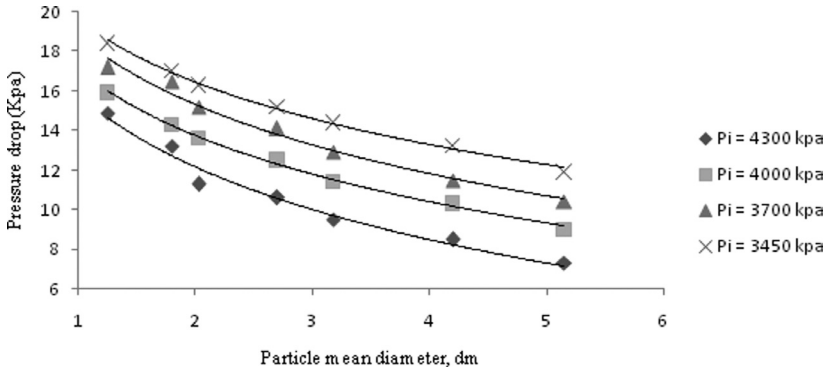

Fig. 4. Effect of particle diameter on the pressure drop for different (P_i).

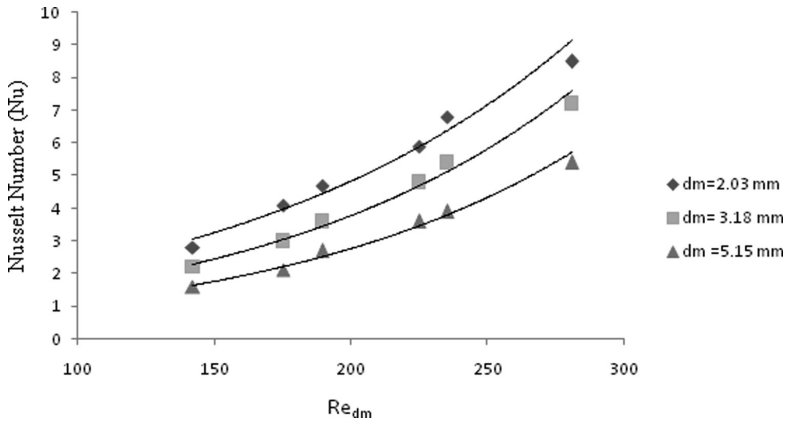

Fig. 5. Effect of Reynolds number on Nusselt number for different particle diameter (d_m).

of the sand decreases (low Darcy number) the heat transfer increases. This is due to the fact that as the porosity decreases the apparent thermal conductivity increases and, accordingly, the heat transfer rate increases. As the permeability of the sand decreases the heat transfer coefficient increases. Also it is clear from this figure that as the inlet pressure increases the heat transfer coefficient increases.

4.5 Effect of Reynolds number and particle diameter on the heat exchanger performance parameter

In the present study and in the design of heat exchangers in which a porous medium is present, a dimensionless parameter is usually used to evaluate the performance based on both the heat transfer enhancement and the associated pressure drop. This parameter is defined according to Hadi Dehghan (2011) as:

$$\varepsilon p = \frac{Nu\Pr^{-2/3}}{f} \tag{19}$$

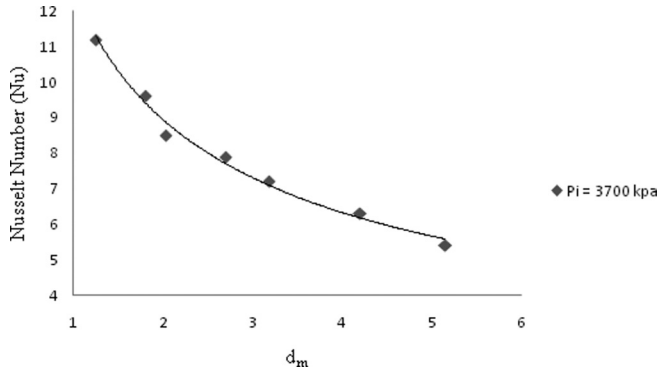

Fig. 6. Effect of particle diameter on Nusselt number.

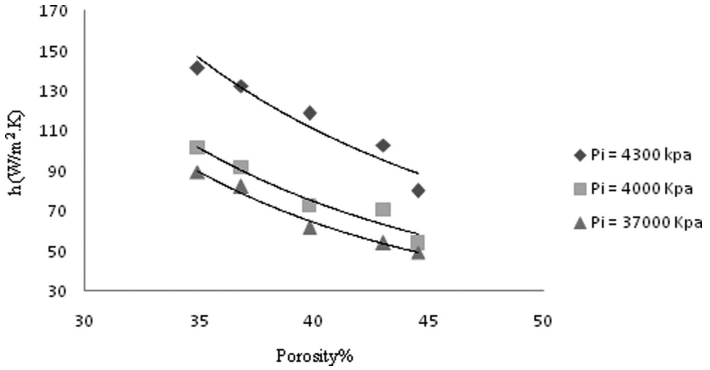

Fig. 7. Heat transfer coefficient versus porosity for different inlet pressures.

where *Nu* is the Nusselt number and is calculated according to the following relation:

$$Nu = \frac{h_i D_e}{k_a} \tag{20}$$

In Fig. 8 the effects of Reynolds number and particle diameter on the heat exchanger performance parameter are illustrated. It can be seen from this figure that as the Reynolds number increases and the particle diameter decreases the heat transfer enhancement increases and the performance parameter decreases. This is due to the fact that the increasing rate of the dimensionless pressure drop is much higher than that of the Nusselt number.

4.6 Effect of porosity on the friction factor in the porous tube

The effect of porosity on the friction factor is depicted in Fig. 9. It can be seen from this figure that as the porosity decreases the friction factor increases due to low permeability and the high resistance of the flow in the porous material.

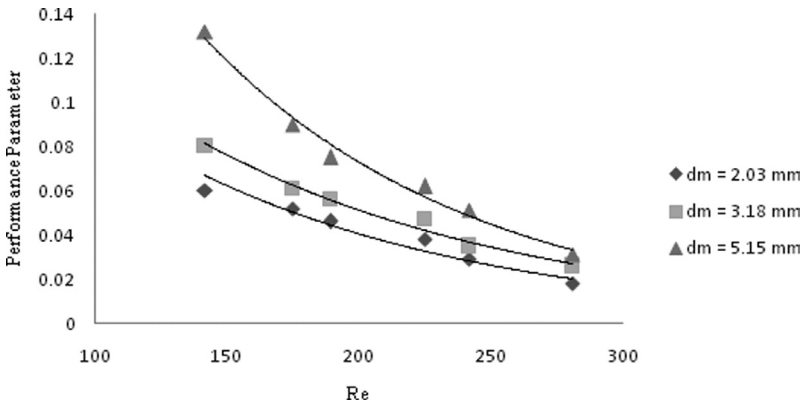

Fig. 8. Effect of Reynolds number on performance parameter for different (d_m).

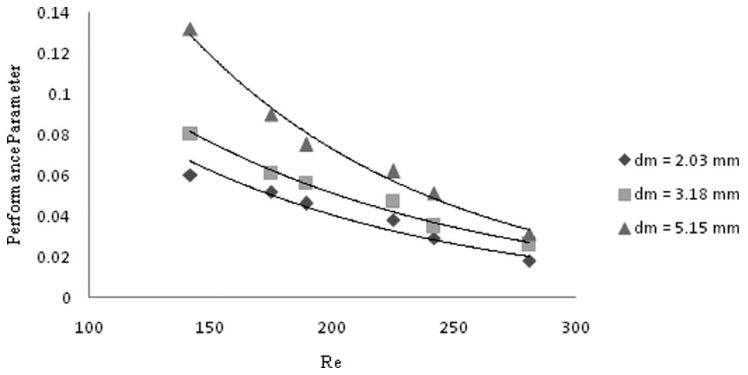

Fig. 9. Friction factor versus porosity for different inlet pressures.

5. Conclusions

An experimental study of single-phase laminar forced convection of carbon dioxide in a single porous tube heat exchanger was conducted. A smaller particle diameter can be used to achieve higher heat transfer enhancement, but a larger particle diameter leads to a more efficient performance based on heat transfer enhancement. The average heat transfer coefficient decreases when the porosity increases. For a large particle diameter (non-Darcy regime), the friction and the corresponding pressure drop both decrease slowly as they approach their corresponding asymptotic values for the nonporous case. Carbon dioxide can be considered a promising working fluid in porous heat exchangers because it has a very low global warming effect and it has zero ozone depletion potential from one side and the ability to enhance the heat transfer coefficient from the other side. This study can be used as a platform in the compact design of heat exchangers.

Literature Cited

1. Alshqirate A, Tarawneh M, Hammad M. The effect of heat exchanger size on two phase heat transfer coefficient, CO_2 case study. The 23rd International Congress of Refrigeration from (21–26) August 2011. Czech Republic.
2. Al-Tarawneh M. Characteristics of CO_2 during condensation and evaporation processes in porous media when used as refrigerant. PhD Thesis. University of Jordan, Amman, Jordan; 2008.
3. Abo-Hijleh BA, Al-Nimr MA. The effect of the local inertial term on the fluid flow in channels partially filled with porous material. Int J Heat Mass Transf 2001;44:1565–1572.
4. Lee D, Vafai K. Analytical characterization and conceptual assessment of solid and fluid temperature differentials in porous media. Int J Heat Mass Transf 1999;42:423–435.
5. Incropera F, Dewitt D, Bergman T, Lavine A. Fundamentals of heat and mass transfer, 6th ed. Wiley & Sons; 2007.
6. Dehghan H, Aliparast P. An investigation into the effect of porous medium on performance of heat exchanger. World Journal of Mechanics 2011;1:78–82.
7. Hammad M, Alshqirate A, Tarawneh M. Cooling of superheated refrigerants flowing inside tubes filled with porous media. Study of heat transfer and pressure drop. Carbon dioxide case study. J Energy Power Eng 2011;5:802–810.

8. Jiang P-X, Xu Y, Lv J, Shi R, He S, Jackson JD. Experimental investigation of convection heat transfer of CO_2 at super-critical pressures in vertical mini-tubes and in porous media. Appl Therm Eng 2004;24:1255–1270.
9. Mills AF. Heat and mass transfer. Irwin; 1995.
10. Alkam MK, Al-Nimr MA. Improving the performance of double-pipe heat exchangers by using porous substrates. Int J Heat Mass Transf 1999;42:3609–3618.
11. Oosthuizen PH, Nayor D. An introduction to convective heat transfer analysis. McGraw-Hill; 1999.
12. Pettersen J, Hafner A, Skaugen G, Rekstad H. Development of compact heat exchangers for CO_2 air-conditioning systems. Int J of Refrig 1998;21(3):180–193.
13. Dias R, Fernands CS. Permeability and effective thermal conductivity of bisized porous media. Int J Heat Mass Transf 2007;50:1295–1301.
14. Sheng-Chung Tzeng, Wei-Ping, Yen-Chan Wang. Friction and forced convective heat transfer in a sintered porous channel with obstacle blocks. Heat Mass Transf 2005;43:687–697.
15. Teamah et al. Numerical simulation of laminar forced convection in horizontal pipe partially or completely filled with porous material. Int J Therm Sci 2011;50:1512–1522.
16. Yoon SH et al. Characteristics of evaporative heat transfer and pressure drop of carbon dioxide and correlation development. Int J Refrig 2004;27:111–119.

□♦ ♦ ♦□